

Application of Tracking Solver for Active Magnetic Bearing Controller Design

Hiroyuki Fujiwara, Makoto Ito, and Osami Matsushita

*Dept. of Mechanical Engineering
National Defense Academy
1-10-20 Hashirimizu, Yokosukai, Kanagawa, Japan
hiroyuki@nda.ac.jp*

Abstract – The tracking solver we propose is defined by sliding mode control theory so that the numerical time history of the solution traces exact values. If one of the initial solutions is provided, the solver calculates all solutions as parameters change from initial to final. The solver solves linear or nonlinear equations. Here we apply it to controller design based on several control design strategies, i.e., direct pole placement, optimal control, and phase adjustment. These control design methods mainly determine control feedback gain and other parameters required for closed-loop behavior of the system. Because this solver obtains gain and parameters as the final condition is selected, control is easier to design. We effectively tuned the controller of an active magnetic bearing using this solver.

Index Terms – tracking solver, optimal control, phase tuning, phase adjustment method, active magnetic bearing

1. INTRODUCTION

When we solve equations using parameters, the solution at each parameter is repeated. It is difficult, however, to continuously identify the changing behavior of each eigenvalue of rotor-bearing systems depending on rotational speed, for example.

We propose a solver defined by sliding mode control theory so that the numerical time history of the solution traces exact values. If one of the initial solutions is provided, the solver calculates all solutions as the parameter changes from initial to final. The solver solves linear or nonlinear equations.

Here we apply the solver to controller design based on several control design strategies, i.e.[1], direct pole placement, optimal control, and phase adjustment. These control design methods mainly determine control feedback gain and other parameters needed for closed-loop behavior of the system. Because the solver obtains gain and parameters as the final condition is selected, the control system is easier to design. We effectively tuned the controller of an active magnetic bearing (AMB) using this solver.

2. TRACKING SOLVER

The tracking solver method is detailed below[2]. The solution, $\lambda(\tau)$, is controlled by the following equation:

$$\dot{\lambda}(\tau) = u \quad (1)$$

We define control force u by a switching function dependent on the error of the output variable on answer planes. Error is written as follows:

$$\sigma = f(\lambda, \tau) \quad (2)$$

The difference is

$$\dot{\sigma} = \frac{\partial f}{\partial \lambda} \dot{\lambda} + \frac{\partial f}{\partial \tau} = \frac{\partial f}{\partial \lambda} u + \frac{\partial f}{\partial \tau} \quad (3)$$

If we select this difference to satisfy the following equation,

$$\dot{\sigma} = -g_1 \text{sign}(\sigma) - g_2 \sigma \quad (4)$$

where $\text{sign}(\sigma) \equiv e^{j\theta}$ ($\sigma = |\sigma|e^{j\theta}$) and g_1, g_2 : high gains

control force is determined by assuming extremely high gains as follows:

$$u = -\left(\frac{\partial f}{\partial \lambda}\right)^{-1} \left(g_1 \text{sign}(\sigma) + g_2 \sigma + \frac{\partial f}{\partial \tau} \right) \quad (5)$$

$$\approx -\left(\frac{\partial f}{\partial \lambda}\right)^{-1} [g \text{sign}(\sigma) + g_2 \sigma]$$

Combining Equation (1) and Equation (5) provides a possible method for the continuous solution $\lambda(\tau)$.

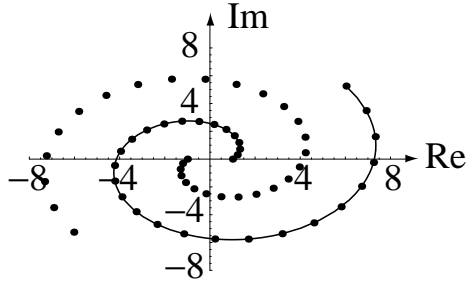
3. CHARACTERISTIC EQUATION

The second-order example equation is as follows:

$$f(\lambda, t) = \lambda^2 - (t+1)^2 e^{2jt} = 0 \quad (6)$$

and we have two answers, $\lambda = \pm(t+1)e^{jt}$. When we apply this solver to Equation (6), the result is as shown in

Figure 1. Each root depending upon the initial condition, $\lambda(0) = \pm 1$, is continuously tracked. In our experience, the selection of improper gains g_1 and g_2 induced the divergence in numerical integration. Case studies in Section 4 chose preferable gains of $g_1 = 10$ to 10^2 and $g_2 = 10^4$ to 10^6 .



Note: \cdot exact — approximate

Figure 1. Solution of tracking solver

4. APPLICATION TO CONTROLLER DESIGN

The common state space equation and control vector are expressed as follows:

$$\begin{aligned} \dot{x} &= Ax + Bu \\ u &= Fx \end{aligned} \quad (7)$$

The controller uses the tracking solver based on several design strategies.

4.1 Direct Pole Placement

Pole placement is done mathematically using a state space representation of the open system and calculating feedback matrix F assigning poles to the desired positions. This paper deals with the following system[3]:

$$A = \begin{pmatrix} -2 & 1 & 0 \\ 1 & -3 & 1 \\ 0 & 1 & -2 \end{pmatrix}, B = \begin{pmatrix} 1 \\ 0 \\ 0 \end{pmatrix}, F_b = \begin{pmatrix} f_1 \\ f_2 \\ f_3 \end{pmatrix} \quad (8)$$

The feedback control loop is constructed to assign poles of a closed-loop system to positions -4 (multiple pole). Eigenvalues of A are $\lambda_{0i} = \{-1, -2, -4\}$ ($i=1,2,3$) and are used by initial values of the tracking solver to satisfy the following equation:

$$chr = \det[sI - A + BF] \quad (9)$$

Eigenvalues of A are $\lambda_{0i} = \{-1, -2, -4\}$ ($i=1,2,3$) and are used by initial values of the tracking solver to satisfy the following equation:

$$\begin{aligned} f(\lambda, \tau) &= chr - ((s - \lambda_{01}) - (\lambda - \lambda_{01})\tau) \\ &\quad \times ((s - \lambda_{02}) - (\lambda - \lambda_{02})\tau) \\ &\quad \times ((s - \lambda_{03}) - (\lambda - \lambda_{03})\tau) = 0 \end{aligned} \quad (10)$$

Error is written as follows:

$$\begin{aligned} \sigma_1 &= \text{the coefficient of } s^2 \text{ in } F \\ \sigma_2 &= \text{the coefficient of } s \text{ in } F \\ \sigma_3 &= \text{the constant term in } F \end{aligned} \quad (11)$$

If $\sigma_1 = \sigma_2 = \sigma_3 = 0$, Equation (10) is satisfied. Figure 2 shows continuous feed back gain, when τ is increased from 0 to 1.0. The desired solution is as follows:

$$F = \{5.0 \ 9.0 \ 13.0\}^t \quad (\tau = 1.0) \quad (12)$$

Eigenvalues $s(= \lambda_i(1.0)) = -4.0$ (multiple poles) are confirmed.

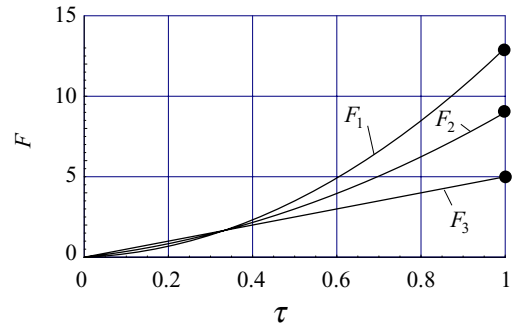


Figure 2 Solutions of pole placement strategy.

4.2 Optimal control

The optimal regulator of the following system is designed to minimize cost functional Equation (14)

$$A = \begin{pmatrix} 0 & 1 \\ 0 & -1 \end{pmatrix}, B = \begin{pmatrix} 0 \\ 1 \end{pmatrix}, F = \begin{pmatrix} f_1 \\ f_2 \end{pmatrix} \quad (13)$$

$$J = \frac{1}{2} \int_0^{\infty} \{x^t Qx + u^t Ru\} dt \quad (14)$$

The control vector is expressed as follows:

$$u = Fx = -R^{-1} B^t Px \quad (15)$$

P is the solution of the Riccati equation[3].

$$A^t P + PA + Q - (PBR^{-1}B^t)P = 0 \quad (16)$$

Assuming $Q = \begin{pmatrix} 1 & 0 \\ 0 & 1 \end{pmatrix}$ and $R = 1$, the Riccati equation is

replaced by the following equation to apply the tracking solver:

$$f(\lambda, \tau) = A^t P + PA + \{Q - (PBR^{-1}B^t)P\}\tau \quad (17)$$

Errors and P are written as follows:

$$\begin{pmatrix} \sigma_1 & \sigma_2 \\ \sigma_3 & \sigma_4 \end{pmatrix} = f(\lambda, \tau)$$

$$P(\tau) = \begin{pmatrix} \lambda_{11} & \lambda_{12} \\ \lambda_{21} & \lambda_{22} \end{pmatrix} \quad (18)$$

When $\tau = 0$, $f(\lambda, 0) = A^t P + PA = 0$. Therefore, the initial value is written as follows:

$$P(0) = \begin{pmatrix} 1 & 1 \\ 1 & 1 \end{pmatrix} \quad (17)$$

Figure 3 shows the continuous solution λ , when τ increases from 0 to 1.0. The desired solution is as follows:

$$P(1.0) = \begin{pmatrix} 2.0 & 1.0 \\ 1.0 & 1.0 \end{pmatrix} \quad (19)$$

Control gain is obtained as follows:

$$F = -R^{-1}B^t P = (1.0 \ 1.0)^t \quad (20)$$

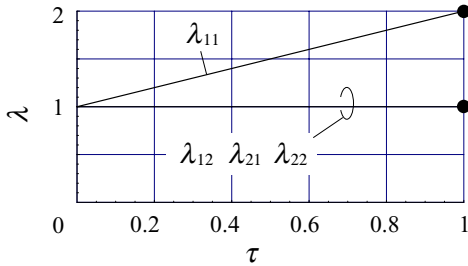


Figure 3 Solutions of optimal control strategy.

5. APPLICATION FOR PHASE ADJUSTMENT

Figure 4(a) shows the 2-degree-of-freedom system that is a reduced model of an AMB, expressed as follows:

$$M = \begin{pmatrix} 0.3 & 0 \\ 0 & 0.7 \end{pmatrix}, K = \begin{pmatrix} 2.8 & -2.8 \\ -2.8 & 2.8 \end{pmatrix} \quad (21)$$

The transfer function of the controller is a phase lead circuit as follows:

$$G_r(s) = g \frac{\tau s + 1}{\alpha \tau s + 1} \quad (22)$$

where $g = 1.0$, $\alpha = 0.5$ and $\tau = 1.5$

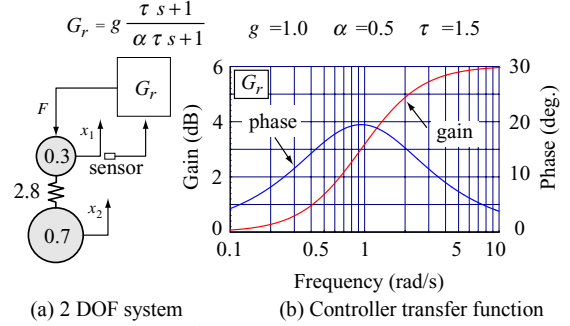


Figure 4 2 DOF system

Figure 4(b) shows the Bode plot of the controller and Figure 5 shows the Bode plot of the open loop transfer function as follows:

$$G_o(s) = G_p(s)G_r(s) \quad (23)$$

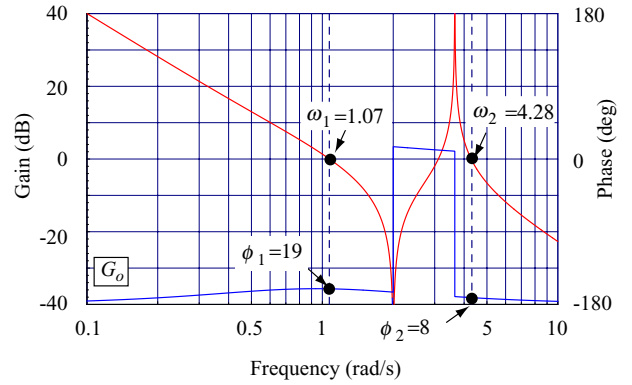


Figure 5 Open loop transfer function of 2 DOF system

To adjust phase and gain, parameters α , τ and g of controller transfer function G_r are tuned. The phase lead $\phi_2 = 9$ at zero cross frequency $\omega_2 = 4.2$ is so small. We tuned parameters so that phase lead ϕ_2 equals 19 (deg). Parameters are determined by the tracking solver. The equation is expressed by the following equation to apply the tracking solver:

$$f_1(\lambda_1, \tau) = \text{Abs}|G_o(j\omega_1)| - 1 \times t \quad (24)$$

$$f_2(\lambda_2, \tau) = \text{Abs}|G_o(j\lambda_4)| - 1 \times t \quad (25)$$

$$f_3(\lambda_3, \tau) = (\text{Arg}|G_o(j\omega_1)| - 19(\text{deg})) t \quad (26)$$

$$f_4(\lambda_4, \tau) = (\text{Arg}|G_o(j\lambda_4)| - 19(\text{deg})) t \quad (27)$$

where $\lambda_1(t) = g(t)$, $\lambda_2(t) = \alpha(t)$, $\lambda_3(t) = \tau(t)$
 $\lambda_4(t) = \omega_2(t)$ and $\omega_1 = 1.07$

Equations (24) and (25) are the condition where gains are 0(dB) at zero cross frequency ω_1 and ω_2 . Equation (26) and (27) are the condition where phase ϕ_1 and ϕ_2 equal 19 (deg) at zero cross frequency ω_1 and ω_2 .

Errors are written as follows:

$$\sigma_i = f_i(\lambda_i, t) \quad (28)$$

where $i = 1, 2, 3, 4$

Initial values are written as follows:

$$\lambda_i = \{0, 0, 0, 4.2(\text{rad/s})\} \quad (29)$$

Figure 6 shows continuous solution λ , when t increases from 0 to 1.0. Controller parameters are obtained as follows:

$$\lambda_i = \{g, \alpha, \tau, \omega_2\} \quad (30)$$

$$= \{1.24, 0.41, 0.65, 4.46(\text{rad/s})\}$$

Figure 7 shows the Bode plot of the open loop transfer function after tuning. The phase lead ϕ_2 at ω_2 is larger than before tuning.

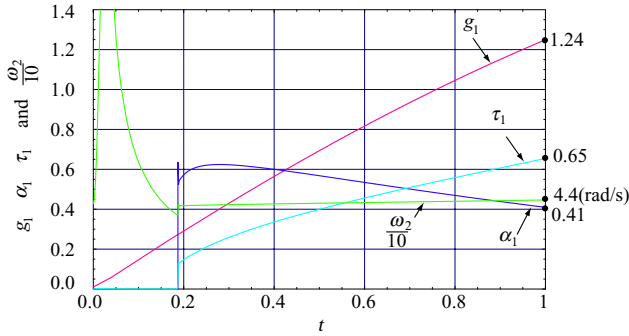


Figure 6 Controller parameters

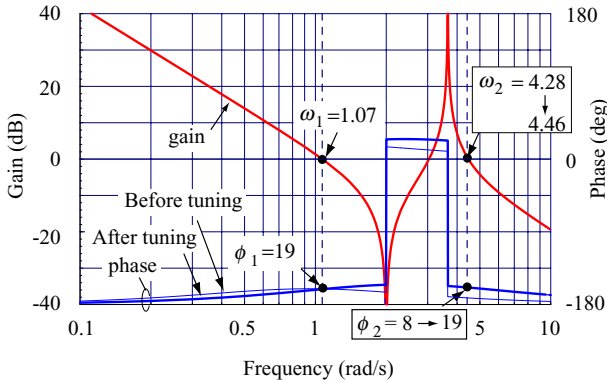


Figure 7 Obtain tuning parameters

6. APPLICATION TO AMB CONTROLLER

6.1 AMB system

Figure 8 gives an overview of the experimental system[4]. The purpose of the three disks at the center and two edge plates of the flexible rotor is to attach rotor correction weights. The disk at the far left is the motor rotor, and the one at the far right is the thrust AMB rotor. The span of the left and right radial AMBs is 1195 mm. Specifications of the flexible rotor are shown in Table 1.

Parameter	Value
Mass (kg)	31.4
Diameter, span (mm)	37, 1316
Material	SUS 304
Rated speed (rps)	250

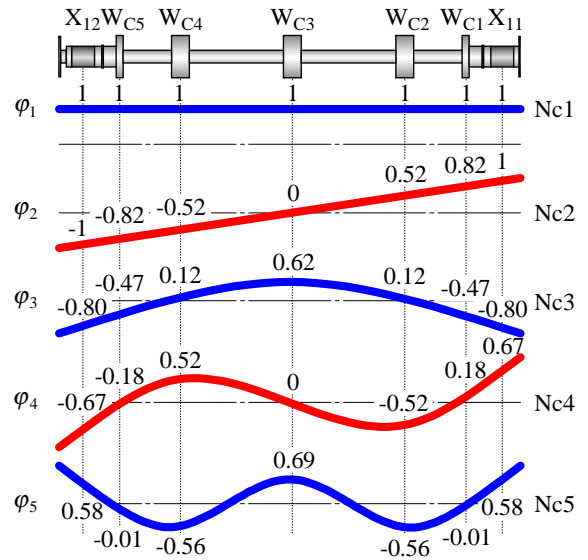
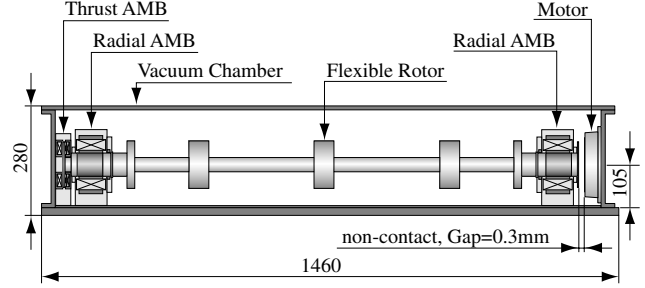


Figure 8 Experimental system and vibration mode

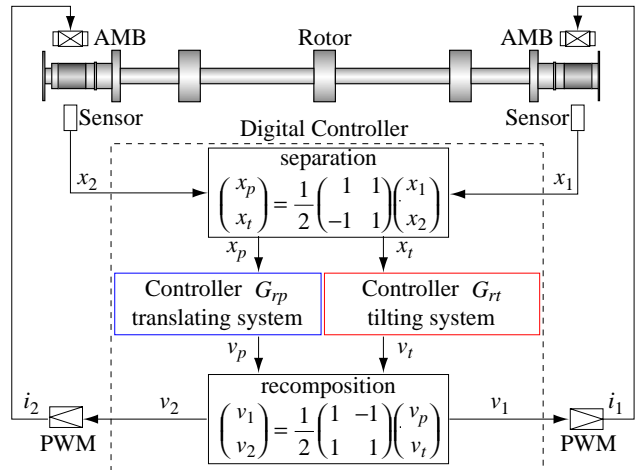


Figure 9 System block diagram

AMBs are controlled digitally by a digital signal processor (DSP). Figure 9 shows a block diagram of the controller of the flexible rotor – AMB. The flexible rotor is symmetrical longitudinally, so the model is controlled by the separation of the translating system and the tilter,

where the translating system is Nc1, Nc3, Nc5... and the tilting system is Nc2, Nc4, Nc6... . The left and right sensor signals captured by the DSP are separated into signals in the translating system and the tilting system through calculation. Signals are calculated at each controller to produce each control output. Each output is sent to the left and right AMBs by repeating calculation. Transfer functions of controllers are as follows:

$$G_{rp}(s) = G_{PID1}(s) \times G_{NF}(s) \quad (31)$$

$$G_{rt}(s) = G_{PID2}(s) \times G_{PSF}(s) \times G_{2LPF}(s) \quad (32)$$

6.2 Unstable vibration

Figure 10 shows the resonance curve up to 260 rps[5]. Amplitude is suppressed by balancing at each mode. However, at 260 rps, a sharp increase in the vibration amplitude is observed at 147 Hz in Figure 11.

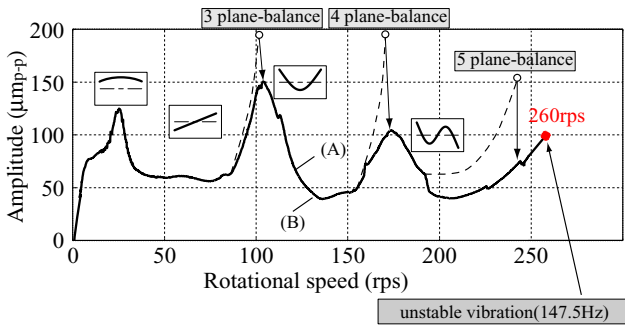


Figure 10 Resonance curve

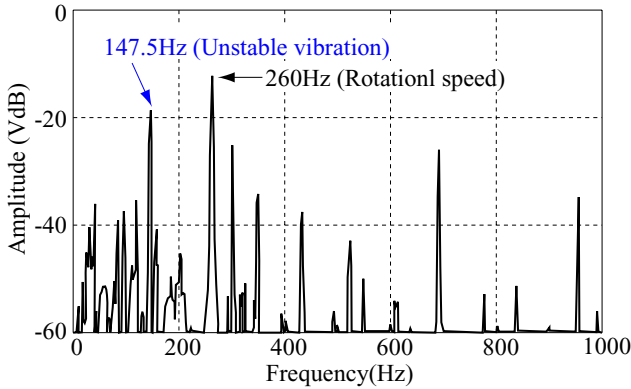


Figure 11 Unstable vibration

The Nc4 backward natural frequency is the probable cause of unstable vibration in the rotational test. Figure 12 shows rotor speed and natural frequency at Nc4. When rotational speed is increased, the natural frequency is separated into two frequencies, called forward and backward natural frequencies. With the measurement of the backward natural frequency with reduced frequency, we found that the natural frequency of 150 Hz is at 250 rps and falls to 140 Hz at the rated speed of 350 rps.

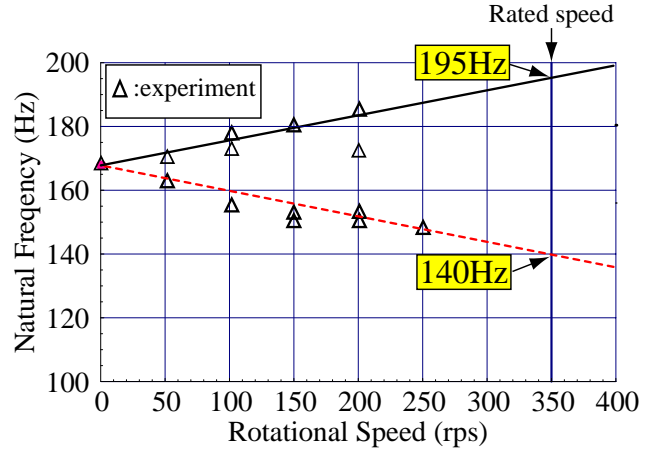
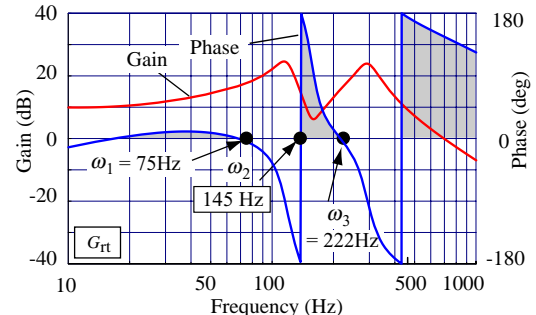


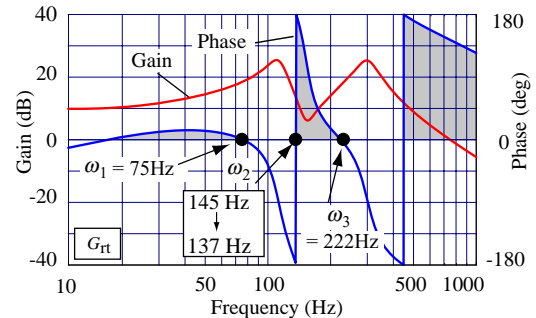
Figure 12 Natural frequency of Nc4 (rotation test)

6.3 Tuning the controller of tilting system

To prevent this unstable vibration, improvements are made to the tilting system controller that controls the second natural bending frequency. Figure 13(a) shows the tilting controller that causes unstable vibration. Phase lag occurs at frequencies below 147 Hz, then the frequency at which the phase is reversed is changed from 147.5 Hz to 137.5 Hz to provide a phase lead at frequencies above 137 Hz in Figure 13(b).



(a) Before controller tuning



(b) After controller tuning

Figure 13 Controller of tilting system

Parameters of the tilting system controller are determined by the tracking solver. The controller transfer function is expressed as follows:

$$G_{rt}(s) = G_{PID2}(s) \times G_{PSF}(s) \times G_{2LPF}(s) \quad (32)$$

where

$$G_{PID2}(s) = 0.5 \left(\frac{240}{\tau_1 s + 1} + \frac{\tau_2 s + 1}{\alpha \tau_2 s + 1} \right)$$

$$\tau_1 = \frac{1}{2\pi \times 0.1}, \tau_2 = \frac{1}{2\pi \times 35}, \alpha = 0.37$$

$$G_{PSF}(s) = \frac{(\tau_4 s)^2 - 2\zeta_2(\tau_4 s) + 1}{(\tau_3 s)^2 + 2\zeta_1(\tau_3 s) + 1}$$

$$\tau_3 = \frac{1}{2\pi \times 123}, \tau_4 = \frac{1}{2\pi \times 163}, \zeta_1 = 0.109, \zeta_2 = 0.084$$

$$G_{2LPF}(s) = \frac{1}{(\tau_5 s)^2 + 2\zeta_3(\tau_5 s) + 1}$$

$$\tau_5 = \frac{1}{2\pi \times 300}, \zeta_3 = 0.12$$

To adjust phase and gain near 140 Hz, the parameters α , τ_3 and τ_4 of G_{PID2} and G_{PSF} are tuned. The equation is expressed by the following equation to apply the tracking solver:

$$f_1(\lambda_1, t) = \text{Arg}|G_o(j\omega_1)| \quad (33)$$

$$f_1(\lambda_2, t) = \text{Arg}|G_o(j\omega_2) - 180(\text{deg})| \quad (34)$$

$$f_3(\lambda_3, t) = \text{Arg}|G_o(j\omega_3)| \quad (35)$$

$$\text{where } \omega_1 = 75 \text{ (Hz)}, \omega_2 = 145 - (145 - 147)t \\ \omega_2 = 222 \text{ (Hz)}$$

$$\lambda_1 = \alpha, \lambda_2 = \frac{1}{2\pi\tau_3}, \lambda_3 = \frac{1}{2\pi\tau_4}$$

Equation (33) is the condition in which frequency ω_1 where the phase is 0 degrees is not changed at 75 Hz. Equation (34) is the condition in which frequency ω_2 where the phase is 180 degree is changed from 147 Hz to 137 Hz. Equation (35) is the condition in which frequency ω_3 where the phase is 0 degree is not changed at 222(Hz).

Errors are written as follows:

$$\sigma_i = f_i(\lambda_i, t) \quad (36)$$

$$\text{where } i = 1, 2, 3$$

Initial values are written as follows:

$$\lambda_i = \{0.37, 123, 163\} \quad (37)$$

Figure 2 shows continuous solution λ , when τ increases from 0 to 1.0. The desired solution is as follows:

$$\omega_2 = 137 \quad (38)$$

Controller parameters are obtained as follows:

$$\lambda_i = \{0.31, 113, 153\} \quad (39)$$

$$\therefore \alpha = 0.3, \tau_3 = \frac{1}{2\pi \times 113}, \tau_4 = \frac{1}{2\pi \times 153}$$

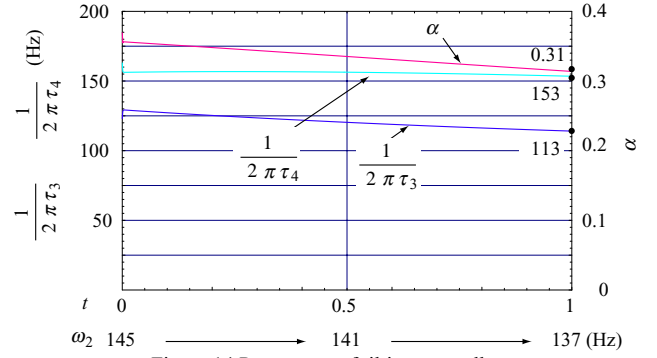


Figure 14 Parameters of tilting controller

After parameters were tuned, the rotational test was done. Figure 15 shows the resonance curve of the rotational test. The rotational speed passes the third critical bending speed Nc5.

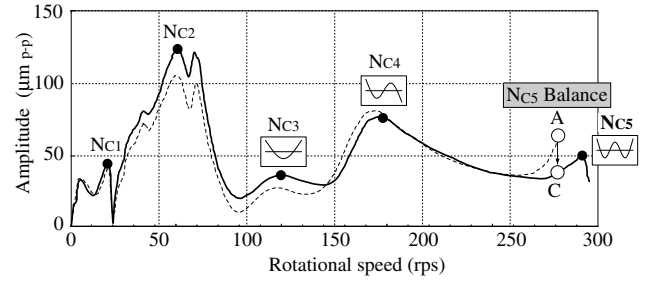


Figure 15 Resonance curve

7. CONCLUSIONS

We have applied our proposed tracking solver to controller design as follows:

- 1) The solver was been applied to controller design based on several control design strategies, i.e., direct pole placement, optimal control, and phase adjustment.
- 2) We tuned the controller of an AMB using this method and designed a stable system for rotation.
- 3) The rotational speed safely passed the third critical bending speed.

REFERENCES

- [1] K. Nonami, K. Den, "Sliding Mode Control", Corona pub., 1994(In Japanese)
- [2] O. Matsushita, H. Fujiwara, M. Ito, "A Tracking Solver Using Sliding Mode Control to Obtain Eigensolutions of Rotor-Bearing Systems," IMechE, pp. 111-120, 2004
- [3] Y. Mori, "Control Engineering", Corona pub., 2001 (In Japanese)
- [4] H. Fujiwara, K. Ebina, M. Ito, N. Takahashi, O. Matsushita, " Control of Flexible Rotors Supported by Active Magnetic Bearings ", Proceedings of the 8th International Symposium on Magnetic Bearings, 2002, pp.145-150
- [5] H. Fujiwara, M. Ito, O. Matsushita and Y. Kanemitsu, " Rotational Test of a Flexible Rotor Supported by Active Magnetic Bearings ", Proceedings of the 2nd International Symposium on Stability Control of Rotating Machinery, 2003, CD-ROM 515